EurJIC
European Journal of Inorganic Chemistry

Research Article
doi.org/10.1002/ejic.202500347

Chemistry Europe
European Chemical Societies Publishing

www.eurjic.org

VIP *Very Important Paper*

Icosahedral Clusters $[In@Tr_{12}]^{10-}$: Synthesis, Characterization, and Electronic Structure Investigations of $Na_4A_6Tr_{13}$ (A = Rb, Cs; Tr = In, Tl)

Melissa Janesch, Antti J. Karttunen, and Stefanie Gärtner*

While thallium forms several clusters in alkali metal thallides, indium clusters in related alkali metal indides are very rare. Here the mixing of the heavy trielides indium and thallium to approximate icosahedral entities present in $Na_4A_6Tr_{13}$ (A = K, Rb, Cs; Tr = In, Tl) is reported. Experimental results prove that at least up to 76% indium can be introduced in this structure type. From the moment indium is provided, the central atom of the icosahedral unit changes from thallium to indium, while the vertices of the cluster are mixed occupied by both, thallium and indium. The bonding and energetics of the compounds are investigated with quantum chemical methods.

1. Introduction

The coordination number of 12 is well-known for element structures built by atoms of the same size, where (anti-)cubeoctahedra are present in cubic and hexagonal closed packed structures, respectively.[1] As soon as differently sized atoms are provided, the icosahedral arrangement becomes more efficient, as the cavity atom in the icosahedron is only ≈90% of the size of the constituents of the latter polyhedron.[2] In this context, icosahedra in general represent very important polyhedra for all aspects of chemistry, as packing requirements are optimized. Even though an icosahedron is the most densely packed arrangement for coordination number 12, the undistorted perfect icosahedral symmetry cannot fill a 3D space with translational symmetry.[3] Thus, it is well-known to be the building unit of quasicrystals.[4] Nowadays, plenty of stable icosahedral quasicrystals are known mostly in different kinds of alloys.[5] Especially for group 13, icosahedral arrangements are of fundamental importance, as these triangulated polyhedra also optimize three-center bonding. While empty icosahedra are known for, e.g., elemental boron,[6] metallic borides,[7] aluminides,[8] gallides[9–11] as well as indides,[12–15] larger icosahedra for thallium result in endohedrally filled entities.[16–19] Recently, it was demonstrated that the size of the Tl_{12} icosahedra influences the occupation of the endohedral position.[20] All these examples have in common that the icosahedra are interconnected to form a 3D network, well-known for classical solid-state compounds.

In contrast, the occurrence of "isolated" icosahedra is commonly assigned to molecular chemistry, especially in $[B_{12}H_{12}]^{2-}$ and its derivatives[21] and also examples for centered transition metal clusters are known.[22] The solid state and the molecular world are combined in Zintl phases,[23] as they allow a salt(-like) description for intermetallic phases. The exploration of group 13 elements with alkali metals revealed a remarkable richness of diverse anionic substructures.[24] Especially for thallium, a vast variety of isolated clusters is known, which usually show very high charges.[25] In this context, two icosahedral entities $[Tl_{13}]^{10-}$ and $[Tl_{13}]^{11-}$ are reported,[16–19,26–30] which can be described as a centered icosahedron. The observation of this structural unit is surprising, as one would expect (anti-) cubeoctahedra for atoms of the same type in this context, the presence of differently sized alkali metals seems to be obligatory. While the closed shell $[Tl_{13}]^{11-}$ is present in the rhombohedrally distorted $Na_3K_8Tl_{13}$ compound (SG no. 166; $R\bar{3}m$), the open shell species $[Tl_{13}]^{10-}$ is observed for the cubic $Na_4A_6Tl_{13}$ (A = K, Rb, Cs) structure type.[17]

Assuming an electron transfer from the less electronegative alkali metal atoms to the more electronegative thallium atoms, which would be in accordance with the Zintl–Klemm–Busmann-concept,[31–33] $Na_4A_6Tl_{13}$ (A = K, Rb, Cs) exhibits a valence electron count (VEC) of 49, which can be considered as hypoelectronic following the Wade–Mingos rules.[34–36] For an optimal icosahedral $[Tl_{12}]^{14-}$ cluster the Wade–Mingos rules.[34–36] would predict 26 ($2n + 2$) skeletal electrons. This would then be isoelectronic to the closo-$[Pb_{12}]^{2-}$, which is only

M. Janesch, S. Gärtner
Department of Inorganic Chemistry
University of Regensburg
93040 Regensburg, Germany

A. J. Karttunen
Department of Chemistry and Materials Science
Aalto University
00076 Aalto, Finland

S. Gärtner
Central Analytics, Faculty for Chemistry and Pharmacy
University of Regensburg
93040 Regensburg, Germany
E-mail: stefanie.gaertner@ur.de

Supporting information for this article is available on the WWW under https://doi.org/10.1002/ejic.202500347

Research Article
doi.org/10.1002/ejic.202500347

known in the gas phase.[37] Centering of this big anionic entity enhances the stability and therefore a vast variety of $[M@Pb_{12}]^{x-}$ clusters are known.[38] Thereby, the central atom can change the electron count depending on the charge of the central atom. The same is true for group 13 elements. While no empty $[Tl_{12}]^{14-}$ clusters are reported until now, thallium-centered thallium icosahedra are well-known. For $[Tl_{13}]^{11-}$ no change in the number of electrons is assumed as a formal Tl^{3+} is added in the center of the icosahedron. But going to the $[Tl_{13}]^{10-}$, which is lacking one electron, an open shell configuration is expected. This is also reflected in the more metallic behavior of the $[Tl_{13}]^{10-}$ cluster compared to the higher charged $[Tl_{13}]^{11-}$. Here, the ideal number of 50 valence electrons for the centered $[Tl_{13}]^{11-}$ icosahedron is observed.

The same is true for $Na_{14}K_6Tl_{18}M$ (M = Mg, Zn, Hg, Cd)[19] and the closely related $Na_{15}K_6Tl_{18}H$,[18] which contain M- or Na-centered icosahedra next to additional octahedral cluster anions. These examples prove, that a change of the central atom allows for the electron count to be adapted. Another possibility to change the electron count comes along with a (partial) structural change as it is observed e.g., in the ternary compound $K_6(NaCd)_2Tl_{12}Cd$, where one sodium position gets mixed occupied with cadmium atoms to raise the VEC. This leads to a certain degree of intercluster bonding and makes the resulting anionic substructure more favorable as the electron count is approximated to the ideal number of 50 valence electrons.[39]

This is in contrast to the lighter trielides indium and especially gallium, which rather form 2D or 3D anionic substructures to reduce the high charges.[10–15,40–44] This results from electronic reasons, as for the lighter trielides, it is generally thought that the *s* electron pair is able to take part in the bonding, as the *s*–*p* separation between the orbitals decreases, while for thallium, the inertness of the 6*s* electron pair prevents this.[45] For anionic thallium clusters, spin-orbit coupling (SOC) and Jahn–Teller (JT) effect induce closed shell electronic configurations.[46]

Interestingly, isolated centered thallium icosahedra could only be observed when alkali metals are mixed, meaning no binary alkali metal thallide, including Tl_{13} is known, as well as no isolated In_{13} cluster has been reported. This raises the following two questions: 1) What is the impact of the different triel elements thallium and indium, respectively? 2) Does the choice of the alkali metal influence the observed substructures?

In the past, mixing of the triels In/Tl was shown to be very fruitful for elucidating the A_2Tr_3 (A = K–Cs; Tr = Ga–Tl) structure types.[40,42–44,47] As we are interested in mixed alkali metal systems and the influence of the latter on the anionic substructure, we investigated the mixture of the heavier trielides thallium and indium in $Na_4A_6Tl_{13}$ (A = Rb, Cs). This is also quite interesting as there is only one additional ternary structure type known–$A_3Na_{26}In_{48}$ (A = Rb, Cs)[15]–for this combination of sodium with the heavier alkali metals rubidium and cesium in the alkali metal indium system. Further, solvation experiments in liquid ammonia were carried out to get an idea about the reactivity of the latter materials toward this solvent. Quantum chemical calculations were performed to investigate the electronic structure, chemical bonding situation, and ground state energy of the compounds.

2. Results and Discussion

Compounds of $Na_4Cs_6Tr_{13}$ (Tr = In, Tl) were first observed in samples of mixing and annealing the binary phases Na_2In and CsTl in different ratios. The powder diffraction pattern showed mainly the diffraction peaks of the starting phases due to incomplete conversion. Hence, the desired compounds were synthesized systematically from the elements in tantalum ampoules, which raised the crystal quality and thus allowed to collect data by single crystal X-ray diffraction (SCXRD). At higher thallium content, the resulting phases were received phase pure, but with increasing indium content, some side phases could be identified (see Supporting Information).

2.1. General Structure Description

The structure type $Na_4A_6Tl_{13}$ (A = K, Rb, Cs)[17] was the first compound reported with that big size of isolated cluster anions among alkali metal trielide systems. It comprises centered $[Tl_{13}]^{10-}$ icosahedra as an exclusive thallium substructure, which are generated by only two crystallographically distinct positions in the cubic space group $Im\overline{3}$. Tl1 atoms on Wyckoff site 2*a* represent the center of the icosahedron, while the icosahedron is formed by symmetry operation *m*. of atom Tl2 on Wyckoff position 24*g*. Even though this anionic $[Tl_{13}]^{10-}$ cluster is referred to as hypoelectronic according to the Wade–Mingos rules[34–36] it is reported to be stable due to packing limitations.[17]

The icosahedron is surrounded by 32 alkali metal atoms in total, eight sodium atoms (all Wyckoff position 8*c*) and 24 rubidium or cesium atoms (all Wyckoff position 12*e*), respectively (see **Figure 1**). All cations bridge between cluster faces or vertices. The 32 heavier alkali metal atoms form a slightly distorted, truncated octahedron around the anionic entities. The eight sodium atoms show a cube-like arrangement around the $[Tl_{13}]^{10-}$ clusters (see **Figure 2**).

In general, icosahedral symmetry cannot be retained in the 230 space groups due to the fact that fivefold symmetry cannot be depicted in a 3D, periodic crystal. Therefore, in cubic $Na_4A_6Tl_{13}$ (A = K, Rb, Cs) they are slightly distorted to T_h symmetry. Also, the Tl–Tl distances in $Na_4A_6Tl_{13}$ (A = K, Rb, Cs) change with the size of the alkali metal but still are in the range of expected Tl–Tl distances.

2.2. Mixing of the Trielides Indium and Thallium

Indium can be inserted in the cubic structure type $Na_4A_6Tl_{13}$ (A = Rb, Cs) up to a certain extent forming a solid solution without observing a substantial change in the crystal structures. Against expectation, but as some examples in literature show,[30,48,49] with increasing indium content the cell parameters increase (see Chapter 3, Supporting Information), while the *Tr*–*Tr* distances decrease (see **Table 1** and **2**).

In the lighter $Na_4Rb_6Tr_{13}$, the Na–*Tr* distances are around 3.15 and 3.17 Å, whereas the Rb1–*Tr*2 distances range between 3.97 and 4.25 Å. Thus, these are comparable to literature known

Research Article
doi.org/10.1002/ejic.202500347

Chemistry Europe
European Chemical Societies Publishing

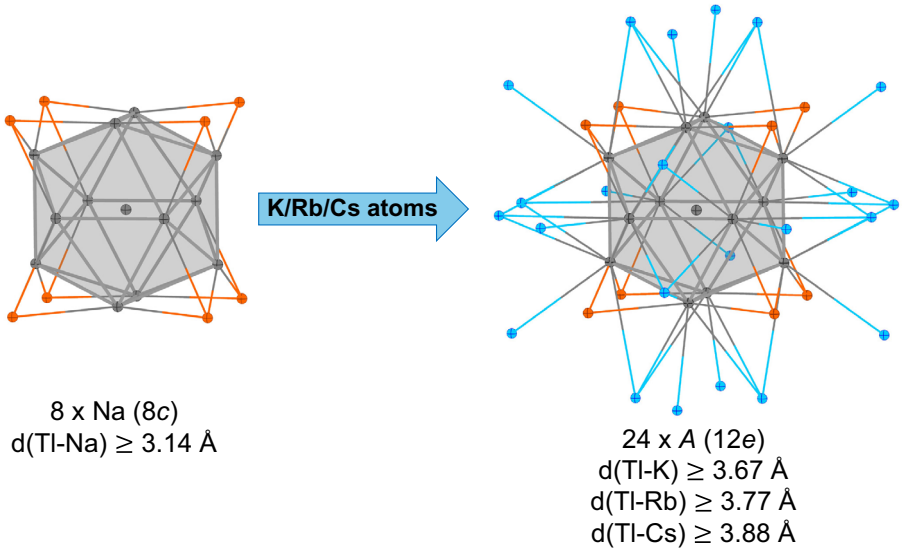

Figure 1. Alkali metal surrounding of the $[Tl_{13}]^{10-}$ clusters. There are eight sodium atoms (Wyckoff position 8*c*) building a cube-like coordination of the icosahedron, while exhibiting a μ^3 coordination of the faces. The 24 heavier alkali metals potassium, rubidium or cesium (Wyckoff position 12*e*) respectively form a truncated octahedron. They coordinate either in a μ^3 fashion or show an end on coordination.

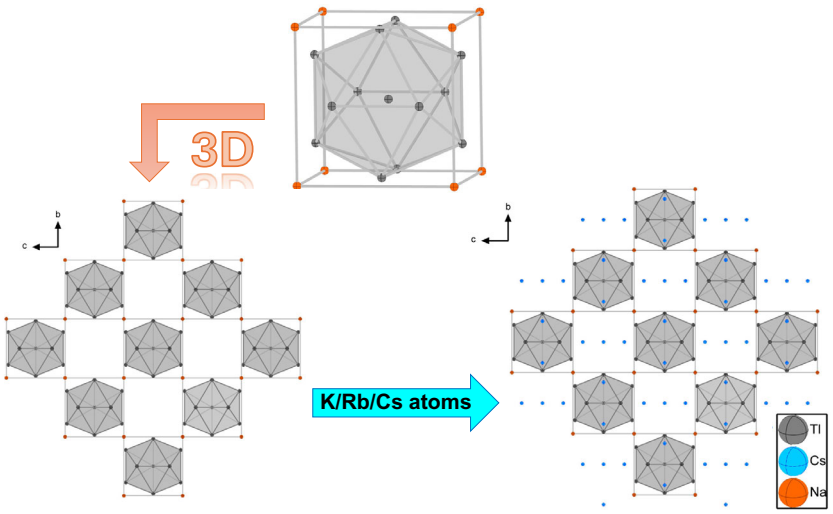

Figure 2. 3D arrangement of the alkali metal atoms in the structure type $Na_4A_6Tl_{13}$ (A = K–Cs). The $[Tl_{13}]^{10-}$ clusters show an AB stacking sequence. Together with the cube-like arrangement of the sodium atoms around them, it reminds of a checkerboard pattern. The heavier alkali metal atom then fills up the voids.

Table 1. Atomic distances and side occupancy factor (s.o.f.) of the icosahedra in the ternary and quaternary phases $Na_4Rb_6Tr_{13}$ (Tr = In, Tl).

	d(*Tr*2–*Tr*2) [Å]	d(*Tr*1–*Tr*2) [Å]	s.o.f.(Tl2)	s.o.f.(In2)
$Na_4Rb_6Tl_{13}$	3.2801(5)–3.4161(3)	3.2225(3)	1	–
$Na_4Rb_6Tl_{10.97}In_{2.03}$	3.2309(4)–3.3645(2)	3.1739(2)	0.914(8)	0.086(8)
$Na_4Rb_6Tl_{9.04}In_{3.96}$	3.2249(3)–3.35618(18)	3.16639(15)	0.749(5)	0.251(5)
$Na_4Rb_6Tl_{7.29}In_{5.71}$	3.2189(4)–3.3524(2)	3.1624(2)	0.609(5)	0.391(5)
$Na_4Rb_6Tl_{6.98}In_{6.02}$	3.2162(3)–3.35022(19)	3.16015(16)	0.581(5)	0.419(5)
$Na_4Rb_6Tl_{5.04}In_{7.96}$	3.2077(2)–3.35022(19)	3.14900(12)	0.420(3)	0.580(3)

structures (see **Table 3**), e.g., in Na_7RbTr_4,[50] which show isolated $[Tr_4]^{8-}$ clusters or in the ternary $Na_3Rb_{26}In_{48}$,[46] where a 3D anionic network is formed. In the heavier solid solution $Na_4Cs_6Tr_{13}$, the alkali metal trielide distances are somewhat longer than with rubidium but also comparable to literature known data (see Table 3).

Research Article
doi.org/10.1002/ejic.202500347

Table 2. Atomic distances and side occupancy factor (s.o.f.) of the icosahedra in the ternary and quaternary phases $Na_4Cs_6Tr_{13}$ (Tr = In, Tl).

	d(*Tr*2–*Tr*2) [Å]	d(*Tr*2–*Tr*2) [Å]	s.o.f.(Tl2)	s.o.f.(In2)
$Na_4Cs_6Tl_{13}$	3.2849(3)–3.4014(2)	3.2123(4)	1	–
$Na_4Cs_6Tl_{11.09}In_{1.91}$	3.2339(2)–3.34423(14)	3.15915(12)	0.924(4)	0.076(4)
$Na_4Cs_6Tl_{9.04}In_{3.96}$	3.2383(3)–3.34848(15)	3.16323(13)	0.753(5)	0.247(5)
$Na_4Cs_6Tl_{7.56}In_{5.44}$	3.2331(3)–3.34355(17)	3.15850(11)	0.612(3)	0.388(3)
$Na_4Cs_6Tl_{5.37}In_{7.63}$	3.2214(3)–3.33018(17)	3.14610(15)	0.453(3)	0.547(3)
$Na_4Cs_6Tl_{3.12}In_{9.88}$	3.2145(3)–3.3181(2)	3.13562(19)	0.261(3)	0.739(3)

Table 3. Atomic distances in the here reported compounds of the quaternary phases $Na_4A_6Tr_{13}$ (A = Rb, Cs; Tr = In, Tl) compared with distances reported in literature.

	d(Na–*Tr*) [Å]	$d_{lit.}$(Na–*Tr*) [Å]	d(*A*–*Tr*) [Å]	$d_{lit.}$(*A*–*Tr*) [Å]
$Na_4Rb_6Tr_{13}$	3.15–3.17	3.17–3.51 (Na_7RbTr_4)[50]	3.97–4.25	3.90–4.21 (Na_7RbTr_4)[50]
		3.23–3.56 ($Na_3Rb_{26}In_{48}$)[46]		3.94–4.13 ($Na_3Rb_{26}In_{48}$)[46]
$Na_4Cs_6Tr_{13}$	3.21–3.24	3.23–3.56 ($Na_3Cs_{26}In_{48}$)[46]	3.86–4.30	4.05–4.98 ($Na_3Rb_{26}In_{48}$)[46]
				3.75–4.41 (CsTl)[28]

As one can see, the Na–*Tr* distances stay in a very close range and do not change a lot as the role of sodium seems to be very important for the formation of this structure type, whereas for the heavier alkali metals, there is a greater leeway in the distances as they can be exchanged.

Substitution of thallium by the lighter homologue indium leads to a change of the endohedral cluster atom. The moment when only a small amount of indium is present in this structure type, $[In@Tr_{12}]^{10-}$ (Tr = In, Tl) clusters are observed, meaning the endohedral atom has changed from a pure thallium to a pure indium position. Something similar is reported for the closely related compound $K_6(NaCd)_2Tl_{12}Cd$. As the atomic radius of cadmium is around 29% smaller than that of thallium,[51] a cadmium atom is implemented in the center of the thallium icosahedron and the Cd–Tl distances decrease compared to the Tl–Tl distances in thallium-centered thallium icosahedra.[39] The same is now true for the here reported solid solution $Na_4A_6Tr_{13}$. When indium is introduced, the *Tr*–*Tr* distances decrease, especially for the *Tr*1–*Tr*2 distances this change is major (see Table 1 and 2). The other way round, if we consider that *Tr*1 position is mixed, it would not be very favorable occupied—from the packing effective side of view—if an indium icosahedron is centered by a thallium atom, which could be supposedly possible if one considers a statistical distribution of the trielide atoms.

What can be observed is the fact that in the solid solution $Na_4Cs_6Tr_{13}$ with the heavier alkali metal cesium, a larger amount of indium can be introduced than in the solid solution $Na_4Rb_6Tr_{13}$. This is considered to be a size effect as the cell parameters increase with increasing indium content (see Chapter 1 and 2, Supporting Information). Further, for the lighter rubidium, a slight decrease of the cell parameters is detected close to a 50:50 ratio of the two trielide atoms. It is assumed that here a slight structural change happens as the former sodium position indicates mixed occupancy with indium (see Chapter 3, Supporting Information). This would mean that the $[In@Tr_{12}]^{10-}$ cluster units get interconnected and as a consequence of indium involvement, the VEC approximates the ideal VEC of 50 (see Chapter 3, Supporting Information).[7,34,35] The same structural feature is reported for $K_6(NaCd)_2Tl_{12}Cd$, where the sodium position shows a mixed occupancy with cadmium to raise the VEC up to 49.7.[39]

2.3. Dissolution Experiments in Liquid Ammonia

Liquid ammonia is known to be the best solvent for highly negatively charged homoatomic species[52] and is able to stabilize new Zintl type clusters. Therefore, dissolution experiments of the two quaternary compounds $Na_4Rb_6Tl_{7.29}In_{5.71}$ and $Na_4Cs_6Tl_{9.04}In_{5.66}$ were carried out. Typically, Zintl anions of group 14 to 16 are reported to be dissolved congruently in liquid ammonia,[53] whereas group 13 elements mostly are oxidized to the elements and alkali metal amide.[27,29] Only recently, the reactivity of alkali metal trielides in this solvent was proven.[49,54]

When liquid ammonia was condensed on the two compounds $Na_4Rb_6Tl_{7.29}In_{5.71}$ and $Na_4Cs_6Tl_{9.04}In_{5.66}$, a colorless solution was observed as well as some black residue at the bottom of the Schlenk flask. After one day, a slightly blue coloring of the solution of $Na_4Cs_6Tl_{9.04}In_{5.66}$ could be observed, while the lighter rubidium-containing compound stayed colorless. After evaporation of the liquid ammonia after 10 weeks, $Na_4Rb_6Tl_{7.29}In_{5.71}$ could be identified in the powder diffraction pattern of the residue (see Chapter 4.7, Supporting Information). For the heavier $Na_4Cs_6Tl_{9.04}In_{5.66}$ elemental thallium and indium, as well as some alkali metal amide, could be indexed next to the unreacted compound (see Chapter 5.6, Supporting Information). These observations indicate a very slow oxidation in liquid ammonia. Further investigations concerning kinetics are in progress.

Research Article
doi.org/10.1002/ejic.202500347

2.4. Electronic Structure Calculations

Different ternary and quaternary compositions of the solid solutions $Na_4A_6Tr_{13}$ (A = Rb, Cs, and Tr = In, Tl) were investigated with the Perdew–Burke–Ernzerhof (PBE) density functional method (DFT-PBE). The compositions were determined by the symmetry of the crystal structure. As there are only two crystallographically independent trielide positions, there are four possibilities for their occupation: 1) all atomic positions can be occupied by thallium ($Na_4A_6Tl_{13}$), 2) all atomic positions can be occupied by indium ($Na_4A_6In_{13}$), 3) the center position can be thallium and the outer one by indium ($Na_4A_6In_{12}Tl$), or 4) the other way round ($Na_4A_6Tl_{12}In$). Two further compositions were also examined by reducing the symmetry from cubic to rhombohedral to get more than one trielide position generating the icosahedron. Thus, the compositions $Na_4Cs_6In_7Tl_6$ and $Na_4Cs_6In_6Tl_7$ could also be investigated. The optimized cell parameters were compared to the experimental ones as far as possible. The deviation between the optimized and experimental cell parameters is around 2%, corresponding to good agreement between theory and experiment. Harmonic frequency calculations did not show any imaginary frequencies, proving the optimized structures to be true local minima (see Supporting Information for the comparison of the lattice parameters).

To get a better insight into the bonding situation of the $Na_4A_6Tr_{13}$ compounds, a Mulliken population analysis was carried out. All tables with the obtained Mulliken populations and the partial charges of each atomic position can be found in the Supporting Information. According to the Zintl–Klemm-Busmann concept[31–33] the alkali metals transfer electron density to the more electronegative trielide atoms, which can be seen in their positive partial charges (from +0.73 up to +0.82 e). No difference between sodium or the heavier alkali metal can be detected. Hence, the more electronegative trielide atoms exhibit slightly negative charges as they receive electron density from the alkali metals. Among the trielide atoms, different partial charges are observed depending on the atomic position of the trielide. The atom on Wyckoff position 24g, which generates the icosahedron, always carries a higher negative charge (from −0.63 up to −0.66 e) than the central atom. Further, for the two existing compounds, $Na_4Rb_6Tl_{13}$ and $Na_4Cs_6Tl_{13}$, as well as for the two compounds $Na_4Rb_6Tl_{12}In$ and $Na_4Cs_6Tl_{12}In$, which are very near to the experimental compositions ($Na_4Rb_6Tl_{10.93}In_{2.07}$ and $Na_4Cs_6Tl_{11.09}In_{1.91}$), both trielide positions exhibit negative partial charges, but the central atom on Wyckoff position 2a shows a negligible negative partial charge (−0.03 e). Going to the hypothetical compounds with more indium, the central atom A exhibits a slightly positive partial charge (from +0.11 up to +0.25 e).

Further, the formation energies, ΔE, of the compounds were calculated. The total electronic energy of both pure elements and the studied compounds was calculated with DFT-PBE (larger TZVP basis sets were needed to describe the elemental alkali metals properly). After optimization, the cell parameters of the elemental alkali metals deviate less than 2% from the experimental ones (see Supporting Information). Then a simple reaction equation was formed according to the synthesis, which is also carried out from the elements (see **Scheme 1**). After that, the formation energy ΔE for each compound can be calculated by comparing the total energy of the compound with the total energies of the constituent elements.

In general, if the formation energy ΔE is negative, it means that the reaction is energetically favorable. For all of our calculated compounds, ΔE was negative (see **Table 4** and additional data in Supporting Information). In Table 4, the reaction energies for the four ternary compounds $Na_4A_6Tr_{13}$ (A = Rb, Cs; Tr = In, Tl) are given. The formation energies of the rubidium-containing compounds are less favorable than for the cesium-containing ones. So, it seems that the heavier cesium compounds could be more likely to form than the rubidium ones.

In **Figure 3** the electronic band structure and density of states (DOS) of $Na_4Cs_6Tl_{13}$ are shown. Further band structure and DOS plots are included in the Supporting Information. The electronic band structure is displayed along high-symmetry directions within the Brillouin Zone (BZ), and the corresponding DOS is decomposed into atomic contributions, yielding the projected (partial) DOS. A metallic character can be assigned to that, as well as to all the other compounds calculated, due to the Fermi level crossing the valence bands. Thus, no bandgap is observed. This metallic character is in line with previous experimental and

1.) $$4\ Na\ +\ 6\ Cs\ +\ 13\ Tl \rightarrow Na_4Cs_6Tl_{13}$$

2.) $$\Delta E = E_{tot}(Na_4Cs_6Tl_{13})\ -\ [4\ x\ E_{tot}(Na)\ +\ 6\ x\ E_{tot}(Cs)\ +\ 13\ x\ E_{tot}(Tl)]$$

Scheme 1. Reaction equation from the elements (1) and the equation for the calculation of the formation energy ΔE (2). For all studied compounds, ΔE is negative meaning that the reaction is energetically favorable.

Table 4. Formation energies ΔE for the ternary compounds $Na_4A_6Tr_{13}$ (A = Rb Cs; Tr = In, Tl) in kJ mol^{-1}. Calculations of the formation energies are based on the reaction from the elements according to synthesis. They are all negative meaning that the reaction is energetically favorable.

Compound	$4xE_{Na}$ [a.u.]	$6xE_{Rb/Cs}$ [a.u.]	$13xE_{Tr}$ [a.u.]	$E_{tot\ elements}$ [a.u.]	$E_{tot\ compoundss}$ [a.u.]	ΔE [kJ mol^{-1}]
$Na_4Rb_6Tl_{13}$	−648.803045	−144.645531	−2243.933300	−3037.381876	−3037.381876	−287
$Na_4Cs_6Tl_{13}$	−648.803045	−121.029327	−2243.933300	−3013.765672	−3013.765672	−319
$Na_4Rb_6In_{13}$	−648.803045	−144.645531	−2472.635528	−3266.084104	−3266.084104	−318
$Na_4Cs_6In_{13}$	−648.803045	−121.029327	−2472.635528	−3242.467900	−3242.467900	−358

Research Article
doi.org/10.1002/ejic.202500347

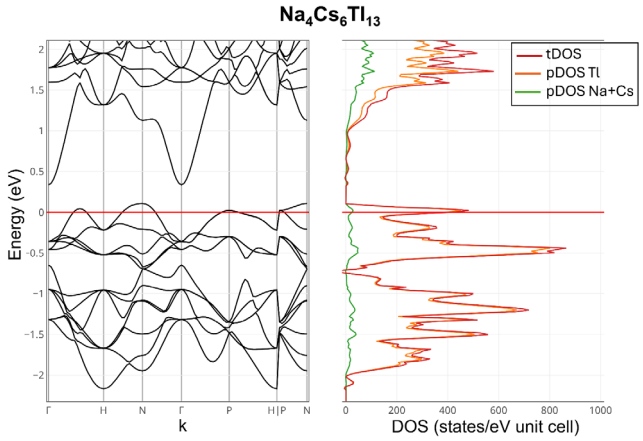

Figure 3. Band structure (left) and density of States (DOS) (right) of the compound $Na_4Cs_6Tl_{13}$. This compound can be synthesized and is already literature reported. As the Fermi level ($E = 0$) cuts through several bands, a metallic character can be assigned to the compound. The DOS is comparted in the total DOS (tDOS) as well as the partial DOS (pDOS) of the two alkali metals cesium and sodium and the pDOS of thallium. As expected, the contribution of the trielide to the tDOS around the Fermi level is much higher than the one for the alkali metals.

computational investigations of Corbett.[17] As shown in the introduction, the rhomboherdally distorted $[Tl_{13}]^{11-}$ cluster exhibits a closed shell configuration and therefore a more salt-like character can be assigned to it compared to the here discussed $[Tl_{13}]^{10-}$ cluster. Thus, this $[Tl_{13}]^{10-}$ cluster is lacking one electron from a closed shell configuration and therefore, the Fermi level crossing the valence bands is reasonable and expected.

3. Conclusion

Mixing of the heavier group 13 elements indium and thallium in the cubic structure type $Na_4A_6Tl_{13}$ (A = Rb, Cs) succeeded in the formation of mixed $[Tr_{13}]^{10-}$ clusters. One striking feature is observed, as in the moment a slight amount of indium is introduced within this system, the endohedral atom of the centered icosahedra changes from a pure thallium to a pure indium position to form $[In@Tr_{13}]^{10-}$ clusters. The formation of the latter is assigned to packing effects. At an indium content of 50%, irregularities in the trends of the unit cell parameters suggest additional effects attributed to a structural change, as detailed investigations of the electron density support a model including intercluster bonding and impressively demonstrate the filigree interplay of packing effects and electronic requirements for the stabilization of alkali metal trielide systems. In general, the results prove that using the bigger alkali metal cesium allows for a higher indium content in this structure type. The compositions of the compounds were also proven by SEM/EDS measurements. Formation energies and Mulliken population analysis from quantum chemical calculations provide some indications, why there is only a certain amount of indium possible in this structure type. Dissolution experiments in liquid ammonia show an oxidation of the trielides to the group 13 elements and alkali metal amides. In summary, mixing of the triel elements in former thallide structures, where isolated clusters are present, represents a powerful tool to approximate still unknown isolated indide clusters in alkali metal compounds. Further investigations on the rhombohedrally distorted $Na_3K_8Tl_{13}$ structure type are ongoing to answer the question, whether, in this case, also fully occupied, endohedral indium can be realized and if the closed shell anionic $[Tr_{13}]^{11-}$ icosahedron might behave differently in dissolution experiments in liquid ammonia.

4. Experimental Section

Materials

Sodium (purity 99%, under mineral oil, Merck/Sigma-Aldrich, Darmstadt) was segregated for purification. Rubidium and cesium were obtained by reduction of RbCl or CsCl respectivley with calcium and afterward purified by two times destillation.[55] Indium drops (purity 99.99%, ABCR) and thallium drops (purity 99.999% ABCR) were used without further purification and were stored under an inert gas atmosphere. Due to the high toxicity of the element thallium, we have a separate fume cupboard, where all instruments, which were used for the work with thallium, were placed. Outside the glovebox, all these instruments as well as the tantalum ampoules are only touched with gloves. Appropriate safety clothing, like a lab coat and goggles, are worn during the work in the laboratory.

Preparation

Due to the fact that the alkali metal indides and thallides are very sensitive toward air and moisture, all operations are performed under an inert gas atmosphere in a glove box (Labmaster 130 G, Fa. M. Braun, Garching, Germany). For the synthesis of $Na_4A_6Tr_{13}$ (A = Rb, Cs, Tr = In, Tl) the elements were placed in a tantalum ampoule, which was sealed in an argon atmosphere. The sealed ampoules were placed in quartz glass tubes (QSIL GmbH, Ilmenau, Germany) and sealed again under argon atmosphere. The following temperature program was used: heating from room temperature to 823.15 K with a heating rate of 100 K h^{-1}, holding for 48 h then cooled with a cooling rate of 100 K h^{-1} to 573.15 K, which were held for 72 h. After that, it was cooled to room temperature with a cooling rate of 3 K h^{-1}.

Solvation Experiments in Liquid Ammonia

In the glove box the compounds were weighted into a Schlenk flask, which was baked out three times before. After that, liquid ammonia was condensed at 195 K on the products using the Schlenk technique. The Schlenk flasks containing the compound with the condensed liquid ammonia were stored at 195 K for one day or 10 weeks, respectively. For evaporation, also Schlenk technique was used again at 195 K. The residue was taken out in the glove box and pestled in a mortar.

X-ray Single Crystal Analysis

A small number of crystals was transferred into vacuum-dried mineral oil. A suitable crystal was selected and mounted on a Rigaku SuperNova diffractometer for $Na_4Cs_6Tr_{13}$ (Rigaku Polska sp. Z. o. o. UI, Wroclaw, Poland) (X-ray: Ag microfocus, AtlasS2 detector) or on a Rigaku XtraLAB Synergy R, DW diffractometer (Rigaku Polska sp.

Z. o. o. UI, Wroclaw, Poland) (rotating anode X-ray tube, Mo Kα radiation, $\lambda = 0.71073$ Å; HyPix-Arc 150 detector) for $Na_4Rb_6Tr_{13}$ using MiTeGen loops. All data were collected at 123 K.

For data collection and data reduction, CrysAlisPro (Version 44_32.144a) was used.[56] The structure solution was carried out with *ShelXT*[57] and for the subsequent data refinement, ShelXL[58] was applied. For visualization purposes, Olex^2 was used and the software Diamond4[59] was chosen for the representation of the crystal structure. All atoms are depicted as ellipsoids with a 50% probability level.

Crystallographic data for the compounds have been deposited in the Cambridge Crystallographic Data Center, CCDC, 12 Union Road Cambridge CB21EZ, UK. Copies of the data can be obtained free of charge under the depository number 2454456, 2454457, 2454459, 2467245, 2467667, 2454460, 2454461, 2454462, 2454463, 2467216 and 2467260, respectively. (Fay: +44-1223-336-033, E-Mail: deposit@ccdc.cam.ac.UK, http://www.ccdc.cam.ac.UK).

Powder Diffraction Studies

Powder diffraction samples were prepared in sealed capillaries (∅ 0.3 mm, WJM-Glas-Müller GmbH, Berlin, Germany). The data collection was carried out on a STOE Stadi P diffractometer (STOE, Darmstadt, Germany) (Monochromatic MoKα1 radiation, $\lambda = 0.70926$ Å) equipped with a Dectris Mythen 1 K detector. For visualization and indexation, the software WinXPOW[60] as well as JANA2006[61] was used.

Quantum Chemical Calculations

The computational studies were carried out using the CRYSTAL23 program package[62] and density functional methods (DFT). The PBE exchange-correlation functional (DFT-PBE)[63] was used. Localized, Gaussian-type triple-ζ-valence + polarization level basis set was used for thallium and indium,[64] split valence polarization level basis set was used for the alkali metals sodium, rubidium, and cesium.[65] For calculations on relative energetics, larger triple-ζ-valence + polarization level basis sets with more diffuse basis functions were used for the alkali metals. The basis sets were derived from the Karlsruhe basis sets[66] (for further details see Supporting Information). For evaluation of the Coulomb and exchange integrals (TOLINTEG), tight tolerance factors of 8, 8, 8, 8, and16 were used for all calculations. The reciprocal space of all compounds was sampled with $3 \times 3 \times 3$ Monkhorst-Pack-type *k*-point grids.[67] For the calculation of the elements, denser *k*-meshes were used (see Supporting Information). Fermi smearing of 0.001–0.002 a.u. (315–630 K) was applied in the electronic structure calculations. The starting geometries were taken either from experimental data or atom positions from known experimental CIFs were modified to get the desired composition, respectively. The lattice parameters and atomic positions were fully optimized within the constraints imposed by the space group symmetry. The optimized structures are provided as Supporting Information. To confirm that the optimized structures were true local minima, harmonic frequency calculations at the Γ-point calculation were carried out to confirm that there are no imaginary frequencies.[68] The Brillouin Zone path Γ–H–N–Γ–P–H |P–N for all compounds of the solid solution $Na_4A_6Tr_{13}$ (A = Rb, Cs; Tr = In, Tl) was provided from the web service SeeK-path.[69]

Supporting Information

The authors have cited additional references within the Supporting Information.[30,31,37]

Acknowledgements

The authors thank Prof. N. Korber and Prof. A. Pfitzner for providing materials and lab equipment. Further, the authors thank Ferdinand Gigl, who performed the SEM/EDS measurement. Financial support by the DFG (Project 468336522), the Rosa-Luxemburg-foundation (M.J.) and the Hans-Böckler-Stiftung (Maria-Weber-Grant for S.G.) is gratefully acknowledged. A.J.K. thanks the Finnish IT Center for Science (CSC) for computational resources.

Open Access funding enabled and organized by Projekt DEAL.

Conflict of Interest

The authors declare no conflict of interest.

Data Availability Statement

The data that support the findings of this study are available in the supplementary material of this article.

Keywords: clusters · density functional method calculations · indium · single crystal X-ray diffraction · thallium

[1] a) A. L. Mackay, *Acta Cryst.* **1962**, *15*, 916; b) M. Jaskolski, B. Naskręcki, Z. Dauter, *ChemTexts* **2025**, *11*, 2.
[2] F. C. Frank, J. S. Kasper, *Acta Cryst.* **1958**, *11*, 184.
[3] a) A. P. Tsai, *Sci. Technol. Adv. Matter* **2008**, *9*, 13008; b) M. Quiquandon, R. Portier, D. Gratias, *Acta Cryst. A* **2014**, *70*, 229; c) E. G. Noya, C. K. Wong, P. Llombart, J. P. K. Doye, *Nature* **2021**, *596*, 367.
[4] a) D. Shechtman, I. Blech, D. Gratias, J. W. Cahn, *Phys. Rev. Lett.* **1984**, *53*, 1951; b) Q. Lin, J. D. Corbett, *Inorg. Chem.* **2003**, *42*, 8762.
[5] A. P. Tsai, in *Physical Properties of Quasicrystals* (Ed: Z. M. Stadnik), Springer Berlin Heidelberg, Berlin, Heidelberg **1999**, pp. 5–50.
[6] B. Albert, H. Hillebrecht, *Angew. Chem.* **2009**, *121*, 8794.
[7] a) V. I. Matkovich, in *Boron and Refractory Borides*, Springer Berlin Heidelberg, Berlin, Heidelberg **1977**; b) N. Vojteer, H. Hillebrecht, *Angew. Chem. Int. Ed.* **2005**, *45*, 165; c) Volker Adasch, Kai-Uwe Hess, Thilo Ludwig, Natascha Vojteer, Harald Hillebrecht, *J. Solid State Chem.* **2006**, *179*, 2900; d) V. Adasch, K.-U. Hess, T. Ludwig, N. Vojteer, H. Hillebrecht, *J. Solid State Chem.* **2006**, *179*, 2150; e) V. Adasch, K.-U. Hess, T. Ludwig, N. Vojteer, H. Hillebrecht, *Chem. Eur. J. Chem.* **2007**, *13*, 3450.
[8] K. J. Nordell, G. J. Miller, *Inorg. Chem.* **1999**, *38*, 579.
[9] C. Belin, M. Tillard-Charbonnel, *Prog. Solid State Chem.* **1993**, *22*, 59.
[10] M. Falk, M. Wendorff, C. Röhr, *Crystals* **2020**, *10*.
[11] R. G. Ling, C. Belin, *Acta Cryst.* **1982**, *B38*, 1101.
[12] B. Li, J. D. Corbett, *Inorg. Chem.* **2006**, *45*, 2960.
[13] W. Carrillo-Cabrera, N. Caroca-Canales, H. G. von Schnering, *Z. Anorg. Allg. Chem.* **1994**, *620*, 247.
[14] W. Carrillo-Cabrera, N. Caroca-Canales, K. Peters, H. G. von Schnering, *Z. Anorg. Allg. Chem.* **1993**, *619*, 1556.
[15] S. C. Sevov, J. D. Corbett, *Inorg. Chem.* **1993**, *32*, 1612.
[16] G. Cordier, V. Müller, *Z. Naturforsch. B* **1994**, *49*, 935.
[17] Z. C. Dong, J. D. Corbett, *J. Am. Chem. Soc.* **1995**, *117*, 6447.
[18] Z.-C. Dong, J. D. Corbett, *Inorg. Chem.* **1995**, *34*, 5709.
[19] Z.-C. Dong, J. D. Corbett, *Angew. Chem. Int. Ed.* **1996**, *35*, 1006.
[20] V. F. Schwinghammer, M. Janesch, F. Kleemiss, S. Gärtner, *Z. Anorg. Allg. Chem.* **2022**, *648*, e202200117.
[21] a) J. A. Wunderlich, W. N. Lipscomb, *J. Am. Chem. Soc.* **1960**, *82*, 4427; b) R. W. Rudolph, *J. Organomet. Chem.* **1976**, *104*, C36.
[22] a) C. E. Housecroft, in *Inorganometallic Chemistry*, (Ed: T. P. Fehlner), Springer US, Boston, MA **1992**, pp. 73–178; b) C. E. Briant,

B. R. C. Theobald, J. W. White, L. K. Bell, D. M. P. Mingos, A. J. Welch, *J. Chem. Soc., Chem. Commun.* **1981**, 201.
[23] G. A. Papoian, R. Hoffmann, *Angew. Chem. Int. Ed.* **2000**, *39*, 2408.
[24] J. D. Corbett, *Angew. Chem. Int. Ed. Engl.* **2000**, *39*, 670.
[25] S. Gärtner, *Crystals* **2020**, *10*, 1013.
[26] a) D. A. Hansen, J. F. Smith, *Acta Cryst.* **1967**, *22*, 836; b) Z.-C. Dong, J. D. Corbett, *Inorg. Chem.* **1996**, *35*, 3107; c) Z.-C. Dong, J. D. Corbett, *J. Am. Chem. Soc.* **1993**, *115*, 11299; d) V. F. Schwinghammer, S. A. Khan, S. M. Tiefenthaler, T. Kovářík, J. Minár, S. Gärtner, *Inorg. Chem.* **2025**, *64*, 6879; e) B. Li, J. D. Corbett, *J. Clust. Sci.* **2008**, *19*, 331; f) S. Kaskel, J. D. Corbett, *Inorg. Chem.* **2000**, *39*, 778; g) G. Cordier, V. Müller, *Z. Krist.* **1992**, *198*, 281; h) S. Gärtner, S. Tiefenthaler, *Proceedings* **2018**, *2*; i) S. Gärtner, S. Tiefenthaler, N. Korber, S. Stempfhuber, B. Hischa, *Crystals* **2018**, *8*, 319; j) Z. Dong, J. D. Corbett, *J. Am. Chem. Soc.* **1994**, *116*, 3429.
[27] V. F. Schwinghammer, M. Janesch, N. Korber, S. Gärtner, *Z. Anorg. Allg. Chem.* **2022**, *648*, e202200332.
[28] Z.-C. Dong, J. D. Corbett, *Inorg. Chem.* **1996**, *35*, 2301.
[29] V. F. Schwinghammer, S. Gärtner, *Inorg. Chem.* **2024**, *63*, 20078.
[30] Z.-C. Dong, J. D. Corbett, *J. Clust. Sci.* **1995**, *6*, 187.
[31] W. Klemm, E. Busmann, *Z. Anorg. Allg. Chem.* **1963**, *319*, 297.
[32] R. Nesper, *Z. Anorg. Allg. Chem.* **2014**, *640*, 2639.
[33] A. Kjekshus, O. Hassel, C. Römming, D. R. Sparrow, *Acta Chem. Scand.* **1964**, *18*, 2379.
[34] K. Wade, *Inorg. Nucl. Chem. Let.* **1972**, *8*, 823.
[35] K. Wade, *Inorg. Nucl. Chem. Let.* **1972**, *8*, 559.
[36] D. M. P. Mingos, *Acc. Chem. Res.* **1984**, *17*, 311.
[37] E. N. Esenturk, J. Fettinger, B. Eichhorn, *Chem. Commun.* **2005**, 247.
[38] a) E. N. Esenturk, J. Fettinger, Y.-F. Lam, B. Eichhorn, *Angew. Chem.* **2004**, *116*, 2184; b) T. F. Fässler, S. D. Hoffmann, *Angew. Chem. Int. Ed.* **2004**, *43*, 6242.
[39] M. Tillard-Charbonnel, C. H. E. Belin, A. P. Manteghetti, D. M. Flot, *Inorg. Chem.* **1996**, *35*, 2583.
[40] M. Falk, C. Röhr, *Z. Kristallogr. Suppl.* **2018**, *38*, 87.
[41] a) B. Li, J. D. Corbett, *J. Am. Chem. Soc.* **2005**, *127*, 926; b) S. C. Sevov, J. D. Corbett, *Inorg. Chem.* **1992**, 1895; c) S. C. Sevov, J. D. Corbett, *J. Solid State Chem.* **1993**, *103*, 114; d) C. Belin, *Acta Cryst. B* **1981**, *37*, 2060; e) R. B. King, *Inorg. Chem.* **1989**, *28*, 2796; f) R. G. Ling, C. Belin, *Z. Anorg. Allg. Chem.* **1981**, *480*, 181; g) S. P. Yatsenko, E. I. Gladyshevsky, K. A. Chuntonov, Y. P. Yarmolyuk, Y. N. Grin, *Kristallografiya* **1983**, *28*, 809; h) J. van Vucht, *J. Less Common Met.* **1985**, *108*, 163.
[42] S. C. Sevov, J. D. Corbett, *Z. Anorg. Allg. Chem.* **1993**, *619*, 128.
[43] S. P. Yatsenko, K. A. Tschuntonow, A. N. Orlow, Y. Yarmolyuk, Y. Hryn, *J. Less Common Met.* **1985**, *108*, 339.
[44] M. Falk, C. Röhr, *Z. Kristallogr.* **2019**, *234*, 623.
[45] F. Wang, G. J. Miller, *Inorg. Chem.* **2011**, *50*, 7625.
[46] a) A. Karpov, M. Jansen, *Chem. Commun.* **2006**, 1706; b) U. Wedig, V. Saltykov, J. Nuss, M. Jansen, *J. Am. Chem. Soc.* **2010**, *132*, 12458; c) V. Saltykov, J. Nuss, U. Wedig, M. Jansen, *Z. Anorg. Allg. Chem.* **2011**, *637*, 357; d) V. Saltykov, J. Nuss, M. Jansen, *Z. Anorg. Allg. Chem.* **2011**, *637*, 1163; e) H. A. Jahn, E. Teller, *Proc. R. Soc. Lond. A* **1937**, *161*, 220.
[47] a) M. Cobián, P. Alemany, A. García, E. Canadell, *Inorg. Chem.* **2009**, *48*, 9792; b) B. Lehmann, *Dissertation*, Albert-Ludwigs-Universität Freiburg, Freiburg, Germany **2023**.
[48] S. C. Sevov, J. D. Corbett, *Inorg. Chem.* **1991**, *30*, 4875.
[49] M. Janesch, V. F. Schwinghammer, I. G. Shenderovich, S. Gärtner, *Z. Anorg. Allg. Chem.* **2023**, *649*.
[50] M. Janesch, K. Gjorgjevikj, S. Krause, S. Gärtner, in preparation.
[51] L. Pauling, *J. Am. Chem. Soc.* **1947**, *69*, 542.
[52] a) E. Zintl, G. Brauer, *Z. Phys. Chem.* **1933**, *20B*, 245; b) E. Zintl, J. Goubean, W. Dullenkopf, *Z. Phys. Chem.* **1931**,*154A*, 1; c) E. Zintl, *Angew. Chem.* **1939**, *52*, 1.
[53] a) S. Gärtner, N. Korber, in *Zintl Ions: Principles and Recent Developments* (Ed: T. F. Fässler), Springer, Berlin Heidelberg, Berlin, Heidelberg **2011**, pp. 25–57; b) *Zintl Ions: Principles and Recent Developments*, (Ed. T. F. Fässler), Springer, Berlin Heidelberg, Berlin, Heidelberg **2011**; c) Chao Liu, Zhong-Ming Sun, *Coord. Chem. Rev.* **2019**, *382*, 32; d) S. Gärtner, M. Witzmann, C. Lorenz-Fuchs, R. M. Gschwind, N. Korber, *Inorg. Chem.* **2024**, *63*, 20240.
[54] C.-C. Yu, A. Ormeci, I. Veremchuk, X.-J. Feng, Y. Prots, M. Krnel, P. Koželj, M. Schmidt, U. Burkhardt, B. Böhme, et al., *Inorg. Chem.* **2023**, *62*, 9054.
[55] L. Hackspill, *Helv. Chimi. Acta* **1928**, *11*, 1003.
[56] M. W. Schneider, I. M. Oppel, A. Griffin, M. Mastalerz, *CrysAlisPRO*, Oxford Diffraction/Agilent Technologies UK, Yarnton, UK **2020**.
[57] G. M. Sheldrick, *Acta Cryst. A* **2015**, *71*, 3.
[58] G. M. Sheldrick, *Acta Cryst. C* **2015**, *71*, 3.
[59] K. Brandenburg, *Diamond*, Crystal Impact GbR, Bonn, Germany **2024**.
[60] A. Toombs, *WinXPOW*, STOE & Cie GmbH, Darmstadt, Germany **2016**.
[61] V. Petříček, M. Dušek, L. Palatinus, *Z. Krist. Cryst. Mat.* **2014**, *229*, 345.
[62] A. Erba, J. K. Desmarais, S. Casassa, B. Civalleri, L. Donà, I. J. Bush, B. Searle, L. Maschio, L. Edith-Daga, A. Cossard, C. Ribaldone, E. Ascrizzi, N. L. Marana, J.-P. Flament, B. Kirtman, *J. Chem. Theory Comp.* **2023**, *19*, 6891.
[63] J. P. Perdew, K. Burke, M. Ernzerhof, *Phys. Rev. Lett.* **1996**, *77*, 3865.
[64] T. M. F. Restle, S. Zeitz, P. M. Stanley, A. J. Karttunen, J. Meyer, G. Raudaschl-Sieber, W. Klein, T. F. Fässler, *Chem. Eur. J. Chem.* **2024**, *30*, e202304097.
[65] a) B. Scheibe, S. I. Ivlev, A. J. Karttunen, F. Kraus, *Eur. J. Inorg. Chem.* **2020**, *2020*, 1319; b) R. E. Stene, B. Scheibe, A. J. Karttunen, W. Petry, F. Kraus, *Eur. J. Inorg. Chem.* **2019**, *2019*, 3672.
[66] F. Weigend, R. Ahlrichs, *Phys. Chem. Chem. Phys.* **2005**, *7*, 3297.
[67] H. J. Monkhorst, J. D. Pack, *Phys. Rev. B* **1976**, *13*, 5188.
[68] a) F. Pascale, C. M. Zicovich-Wilson, F. López Gejo, B. Civalleri, R. Orlando, R. Dovesi, *J. Comp. Chem.* **2004**, *25*, 888; b) C. M. Zicovich-Wilson, F. Pascale, C. Roetti, V. R. Saunders, R. Orlando, R. Dovesi, *J. Comp. Chem.* **2004**, *25*, 1873.
[69] Y. Hinuma, G. Pizzi, Y. Kumagai, F. Oba, I. Tanaka, *Comp. Mat. Sci.* **2017**, *128*, 140.

Manuscript received: July 7, 2025
Revised manuscript received: August 25, 2025
Version of record online: